# CD8 T cells mediate direct biliary ductule damage in NOD autoimmune biliary disease

**Guo-Xiang Yang**[1], **Yuehong Wu**[2], **Hiroki Tsukamoto**[2], **Patrick S. Leung**[1], **Zhe-Xiong Lian**[1], **Daniel B. Rainbow**[4], **Kara M. Hunter**[4], **Gerard A. Morris**[4], **Paul A. Lyons**[4], **Laurence B. Peterson**[3], **Linda S. Wicker**[4], **M.E. Gershwin**[1], and **William M. Ridgway**[2]

[1]Division of Rheumatology, Allergy and Clinical Immunology, University of California at Davis, Davis CA 95616

[2]Division of Immunology, Allergy and Rheumatology, University of Cincinnati College of Medicine, Cincinnati, Ohio, 45267

[3]Deparment of Pharmacology, Merck Research Laboratories, Rahway, NJ 07065

[4]Juvenile Diabetes Research Foundation/Wellcome Trust Diabetes and Inflammation Laboratory, Department of Medical Genetics, Cambridge Institute for Medical Research, University of Cambridge, Cambridge CB2 0XY, UK

## Abstract

We previously described the NOD.c3c4 mouse, which is protected from type 1 diabetes (T1D) due to protective alleles at multiple insulin-dependent diabetes (*Idd*) genes, but develops autoimmune biliary disease (ABD) resembling primary biliary cirrhosis (PBC). Here we characterize the NOD.ABD strain, which is genetically-related to the NOD.c3c4 strain but develops both ABD and T1D. Histologically, NOD.ABD biliary disease is indistinguishable from that in NOD.c3c4 mice. The frequency of effector memory ($CD44^+CD62L^-$) and central memory ($CD44^+CD62L^+$) CD8 T cells is significantly increased in the intrahepatic lymphocyte fraction of NOD.ABD mice, and NOD.ABD CD8 T cells produce more IFN-γ and TNF-α, compared to controls. NOD.ABD splenocytes can transfer ABD and T1D to NOD.c3c4 *scid* mice, but only T1D to NOD *scid* mice, suggesting that the genetic origin of the target organ and/or its innate immune cells is critical to disease pathogenesis. The disease transfer model, importantly, shows that biliary duct damage (characteristic of PBC) and inflammation precede biliary epithelial cell proliferation. Unlike T1D where both CD4 and CD8 T cells are required for disease transfer, purified NOD.ABD CD8 T cells can transfer liver inflammation into NOD.c3c4 *scid* recipients, and disease transfer is ameliorated by co-transferring T regulatory cells. Unlike NOD.c3c4 mice, NOD.ABD mice do not develop antinuclear or anti-Smith autoantibodies; however, NOD.ABD mice do develop the anti-pyruvate dehydrogenase antibodies typical of human PBC. The NOD.ABD strain is a model of immune dysregulation affecting two organ systems, most likely by mechanisms that do not completely coincide.

Current address for Laurence B. Peterson: Hoffmann-La Roche, Inc., Inflammation Discovery, 102/B317, 340 Kingsland Street, Nutley, NJ 07110, U.S.A.

## Keywords

NOD.ABD mice; Adoptive transfer; Primary biliary cirrhosis; Type 1 diabetes

## Introduction

Primary biliary cirrhosis (PBC) is an autoimmune liver disease characterized by a progressive portal lymphocytic inflammatory response and destruction of intrahepatic bile duct epithelial cells (1). A serologic hallmark of PBC is the presence of autoantibodies reactive with the subunits of the mitochondrial 2-oxoacid dehydrogenase complexes, particularly the E2 subunit of the pyruvate dehydrogenase complex (PDC-E2) (1–4). This anti-mitochondrial antibody is a key diagnostic marker in PBC, and can precede disease onset by several years (5). CD4 and CD8 T cell epitopes specific for PDC-E2 have been demonstrated in PBC patients, indicating autoreactive T cells are important in the development of PBC (6–8). However the precise nature of the autoimmune effector mechanisms of biliary ductular damage remains unclear, partly due to the inherent difficulty in studying primary cellular events during the early, asymptomatic phase of PBC and the general limitations of human-based research (9–13).

Recently, we and others have developed novel mouse models of PBC. Each model has similarities and differences from human PBC. The NOD.c3c4 mouse develops an autoimmune biliary disease resembling PBC. It is a congenic strain developed on the genetic background of the nonobese diabetic (NOD) mouse, which is a model of autoimmune diabetes. NOD.c3c4 mice spontaneously develop a severe autoimmune biliary disease with progressive portal inflammation, histological features similar to those found in PBC, and variable penetrance of PDC-E2 antibodies (14–15). In contrast to human PBC, however, the NOD.c3c4 mouse also develops CBD dilation and biliary epithelial cell proliferation (15). The disease can be ameliorated, with modulation of biliary epithelial cell proliferation/portal inflammation, by treatment with anti-CD3. Notably, due to protective alleles at multiple *Idd* genes present in the non-NOD chromosome 3 and 4 congenic regions, NOD.c3c4 mice do not develop T1D. Additional mouse models of PBC were generated in IL-2Ralpha$^{-/-}$, TGF-beta receptor II dominant negative (dnTGFβRII) mice, and NOD congenic mice infected with *Novosphingum aromaticivorans* (16–17). All of these models show varying degrees of portal inflammation and PDC-E2 autoantibody penetrance.

The existence of several different models allows further studies into the pathogenesis of PBC. It is clear from the above studies that immune regulation plays a large role in pathogenesis in the animal models of PBC. In this paper, we have derived a new congenic model of PBC, NOD.ABD, from the NOD.c3c4 mouse. We show that the NOD.ABD strain has much reduced B6- and B10-derived congenic segments on chromosomes 3 and 4, respectively, compared to the NOD.c3c4 mouse, but develops similar biliary disease. In addition, NOD.ABD mice also develop T1D whereas NOD.c3c4 mice do not. T1D and ABD in NOD.ABD mice may have distinct mechanisms of organ specific autoimmune disease pathogenesis.

## Material and Methods

### Animals

NOD.ABD, NOD.B6 *Idd10/18*, B10.*H2$^{g7}$*, NOD.c3c4-*scid*, and NOD-*scid* mice were maintained at Taconic, Inc. and housed under specific pathogen-free conditions at the University of California (Davis, CA), the University of Cincinnati (Cincinnati, OH), or Merck Research Laboratories (Rahway, NJ). All studies were performed with approval from the Animal Care and Use Committees of the University of California, the University of Pittsburgh, The University of Cincinnati, or Merck Research Laboratories.

The NOD.ABD strain was originally developed to test the ability of the chromosome 4 region encoding type I interferons, which is polymorphic between the B10 and NOD strains, to modify the frequency of type 1 diabetes in the NOD mouse in the context of genetic protection from T1D mediated by protective B6-derived alleles at *Idd10* and *Idd18* on chromosome 3 in the NOD.B6 *Idd10/18* strain (referred to as Taconic lines 1101 and 7754 in Fraser *et al.*) (18) (Fig. 1A). The B10-derived type I IFN region is present in the NOD.c3c4 congenic strain, a mouse strain that has been shown to be completely protected from diabetes by virtue of the large non-NOD gene regions on chromosomes 3 and 4 derived from diabetes-resistant strains. However, NOD.c3c4 mice do develop ABD apparently caused by an unfortunate combination of genes derived from the non-NOD strains and the NOD background (14, 15, (19).

The NOD.ABD (N8) strain was developed from the NOD.c3c4 strain following an intercross with the NOD.B6 *Idd10/18* congenic strain (Fig. 1A), and selection of a recombinant mouse having a chromosome 4 congenic segment including the type I IFN region. Mice homozygous for both the B6-derived *Idd10/18* region and the B10-derived type I IFN regions were selected by further intercrossing. Soon after the establishment of the NOD.ABD line, it was discovered that the mice developed autoimmune biliary disease.

After the development of the NOD.ABD strain, the NOD.ABD and NOD.c3c4 congenic strains were defined more precisely by genotyping DNA samples using a 5K mouse SNP chip. The assay, performed by ParAllele Biosciences (South San Francisco, CA), revealed that the NOD.ABD and NOD.c3c4 strains have a small number of non-NOD SNPs outside of the defined congenic regions, one region of non-NOD SNPs on chromosome 1 and another on chromosome 18. New congenic strains are in development to assess the contribution of these non-NOD regions on chromosomes 1 and 18 to the phenotypes described in this manuscript.

### Histopathology scoring

Histological sections were prepared by H&E. The slides were read for 1) biliary duct involvement (i.e. how many portal triads were diseased as indicated by biliary epithelial proliferation and leucocytic infiltration), 2) biliary epithelial proliferation (i.e. the extent of biliary epithelial proliferation / cyst formation), and 3) mononuclear leucocytic infiltration, by a blinded observer. For duct involvement the score was assessed as percent of ducts affected as follows: "0" = <5%, "1"= 5-25%, "2"= 25-50%, "3" = >50%. For biliary epithelial proliferation the slides were scored as follows: 0 = no abnormal proliferating

ductules; "1" = a few (1-4) abnormal proliferating ductules; "2" = multiple (>5) small ductules per triad; "3" = multiple ductules per triad and also many enlarging ductules ("cysts"); "4" = dilated, diffuse, torturous ducts ("cysts") in much of the section. Mononuclear leucocytic infiltration was scored as follows: "0" = none or a few cells; "1" = small numbers of cells in multiple areas; "2" = small numbers of cells (infiltrate a few cells thick) diffusely; or patchy moderate infiltrates; "3" = moderate numbers of cells diffusely or patchy large infiltrates; "4" = diffuse or significant sections of large cellular infiltrates.

## Common bile duct (CBD) and liver gross pathological scoring

CBD dilation and the quantitation of liver abnormalities were examined and scored separately. The CBD score was assigned as follows: "0" normal, less than 1 mm; "1" CBD diameter minimally dilated, 1-2 mm diameter; "2" CBD clearly enlarged, 2-3 mm diameter; "3" CBD clearly enlarged, 3-4 mm diameter; "4" CBD very enlarged, >4 mm diameter. The liver score was assigned as follows: "0" normal; "1" very few lesions in the liver detectable; "2" lesions in liver easily noticed; "3" many liver lesions easily seen; "4" many lesions in most or all lobes; "5" liver completely full of lesions.

## Adoptive transfer protocol

For adoptive transfer experiments, $40 \times 10^6$ splenocytes from diseased male and female NOD.ABD mice were transferred into sex-matched NOD.c3c4-*scid* or NOD-*scid* recipients, age 42-60 days old. The recipients were aged for 30-60 days (or until diabetic) following transfer, sacrificed, scored for gross liver disease, then livers were extracted and examined histologically for disease. Serum from recipients was also used for autoantibody analysis. In separate experiments, specific cell subsets were purified from the spleens of diseased NOD.ABD donors by either FACS sorting or magnetic bead separation (MiniMACS, Miltenyi Biotec, Auburn CA) and transferred into NOD.c3c4-*scid* recipients as described (20).

## ANA Immunofluorescence and Protein immunoprecipitation

Prepared HEP-2 slides were purchased from Diasorin (Stillwater, Minnesota). Mouse sera were diluted 1:20 in 10 mM PBS pH 7.3. 25 μl of the diluted sera was incubated on the slide for 30 minutes in a dark moist chamber and washed in 10 mM PBS in a Coplin jar for 10 minutes. Fluorescein conjugated goat antibody to mouse IgG, IgM, and IgA (ICN Biomedicals, Costa Mesa, California) was diluted 1/100 in PBS. 35μl of the diluted conjugate was placed on each well and the slide was incubated 30 minutes in a dark moist chamber and washed in PBS for 10 minutes. Slides were viewed and scored at 400x magnification with a dry lens of a Leitz fluorescence microscope equipped with a mercury vapor lamp. Protein immunoprecipitation for detection of anti-Smith antibodies was performed as previously described (15). Briefly, rapidly growing, undifferentiated K562 cells were grown at 37°C and 5% $CO_2$ in DMEM supplemented with 10% fetal bovine serum (FBS). Cells were collected in 200 ml conical tubes, centrifuged at 800 rpm for 8 minutes, washed once with pre-warmed methionine-free DMEM culture media and centrifuged again. The medium was removed and for each sample the following were added: 5 ml methionine- free DMEM supplemented with 3% FBS, 50 μCi $^{35}$S methionine (ExpreSS, New England Nuclear, Boston, Massachusetts) and $1 \times 10^6$ K562 cells. The cells

were labeled at 37°C overnight (8-16 hours), collected, washed, and suspended in 5-10 ml IP buffer: 10mM Tris/HCl pH 8.0, 500 mM NaCl, 0.1% Igepal. They were then sonicated, and the sonicate was centrifuged for 10 minutes at 4°C at 14,000 rpm to remove debris. A 10 μl serum sample was bound overnight to 2 mg Protein A Sepharose CL4b beads (Pharmacia), washed three times with IP buffer and incubated two hours at 4°C with the $^{35}$S methionine radiolabeled extract from approximately 1 x10$^6$ rapidly dividing K562 cells. The beads were washed 3 times with IP buffer, suspended in 2x Laemmli sample buffer, loaded on a standard size 8%-15% SDS-PAGE gel with a 5% stack and electrophoresed at 200V. The gels were enhanced by soaking for 30 minutes in 0.5 M sodium salicylate. The gels were dried and autoradiographed 2-7 days. Apparent molecular weights of positive bands were determined by plotting the molecular weight of known $^{14}$C- labeled standards run on the same gel. The eight polypeptide components of snRNPs associated with anti-Smith immunoprecipitation (A, B, B', C, D, E, F, and G) were identified by molecular weight and distribution after immunoprecipitation by comparison to control positive sera (from known anti-Smith positive NOD.c3c4 mice).

### Isolation and flow cytometric analysis of liver T cells

NOD.ABD and control B10.$H2^{g7}$ mice (which have the NOD MHC on the B10 background but do not develop T1D or ABD) were examined at serial ages and liver lymphoid cells isolated as described previously (21). Briefly, PBS-perfused livers were passed through a 100-μm nylon cell strainer (BD Bioscience, Bedford, MA). Lymphocytes were separated from hepatocytes by centrifugation with Histopaque-1.077 (Sigma-Aldrich, St. Louis, MO). Single cell suspensions were washed and viability confirmed using trypan blue exclusion. For flow cytometry, Fc receptors were blocked by incubation with the 2.4G2 mAb (eBioscience, San Diego, CA) and cells stained with fluorochrome-conjugated Abs at 4°C in PBS/0.2% BSA for 30 min. The Abs for TCRβ, CD4, CD8, CD44, CD25, and CD62L were purchased from eBioscience; CD11b, Gr-1, F4/80, Dx5, and CD19 from BD biosciences. Granulocytes were defined as CD11b+, Gr-1$^{high}$, and F4/80-; Macrophages were defined as F4/80+ and CD11b+. NK cells were defined as TCR-Dx5+. NKT cells were defined as CD4+ or CD4- TCR$^{intermediate}$; this was confirmed by staining with alpha gal-cer FITC (not shown). B cells were defined as CD19+. Foxp3 intracellular staining kit was purchased from eBiocience and cells stained following the protocol provided by the company. Stained cells were subjected to multiple-color flow analyses using a FACScan flow cytometer updated by Cytec Development (Fremont, CA) to allow for 5-color analysis.

### *in vitro* cell stimulation

Splenic lymphocytes were purified by centrifugation with Histopaque-1.077 (Sigma-Aldrich, St. Louis, MO). Lymphocytes were incubated with anti-CD4 or anti-CD8 magnetic microbeads for 15 min, washed, and collected on a magnetic flow-through column. Purified cells were suspended in complete medium consisting of RPMI 1640 (with glutamine) supplemented with 10% (wt/vol) FCS, 100 U/ml penicillin and 100 μg/ml streptomycin (Life Technologies). Cells were then transferred into 96-well plates precoated with 10 μg/ml anti-CD3 antibody and 1 μg/ml anti-CD28 antibody (BD Biosciences). The cells were cultured for 72 h at 37°C in a humidified 5% CO2 atmosphere. The supernatants were collected at the end of culture and stored at -70°C.

## Measurement of serum cytokines

Serum samples were collected from NOD.ABD mice at serial age points and stored at -70°C until assayed. Concentrations of IFN-γ and TNF-α in sera or in supernatants of cultured T cells were measured simultaneously with a mouse inflammatory cytometric bead array (CBA) kit (BD Biosciences). Samples were analyzed on a FACScan flow cytometer (BD Immunocytometry Systems) using cytometric bead array software (BD Biosciences).

## Measurement of intracellular interferon gamma

For intracellular IFN-γ staining, liver lymphoid cells were suspended in complete culture medium ($1\times10^6$ cells/ml) and seeded in a 24-well plate ($1\times10^6$ cells/well). Cells were stimulated with 0.5 μg/ml anti-CD3 and anti-CD28 antibody. BFA (10 μg/ml) was added to the culture during the last 6 hours of incubation. After 24 hours of culture, cells were collected and washed one time with PBS/0.2% BSA, and stained with Abs for CD4, CD8, and TCRβ as above. The surface stained cells were permeabilized, and stained with FITC-conjugated anti-IFN-γ mAb for 30 mins at 4°C (BD Biosciences). Stained cells were analyzed using flow cytometry.

## Immunoblotting

10 μg of purified recombinant PDC-E2 was resolved on a 10% Novex mini gel (Invitrogen, Carlsbad, CA). The proteins were electro-blotted to nitrocellulose membrane (Whatman, Dassel, Germany) and cut into 2 mm strips. Each strip was then blocked for 1 hour at room temperature (RT) with casein blocker (Piece Biotechnology, Rockford, IL). The strips were incubated for 1 hour with either mouse sera (1:200) or an anti-mitochondrial positive human PBC control serum (1:1,000) or a mouse anti-PDC-E2 monoclonal antibody, 2H4 (22–23) (1:50) diluted in PBS containing 0.05% Tween-20 (PBS-T) and 0.05% casein blocker (Fisher Biotech, Fair Lawn, NJ). The strips were then washed 6 times for 5 minutes in PBS-T. The secondary antibody was either horseradish peroxidase (HRP)-conjugated goat anti-mouse immunoglobulin G, A, M (IgG, A, M) or HRP-conjugated goat anti-human IgG, A, M (Zymed, San Francisco, CA) diluted 1:10,000 in the same solution as the primary antibody. The strips were exposed for 1 hour at RT to the respective secondary antibodies followed by 6 PBS-T wash cycles and exposed for 5 minutes to chemiluminescent substrate (Piece Biotechnology). Reactive components were visualized with a Fluor Tech 8900 gel doc system (Alpha Innotech, San Leandro, CA) equipped with a chemiluminescent filter.

## Statistical analysis

An unpaired, two-tailed Student's t-test was used for comparison of weight, cell number, cell type frequencies, and cytokine levels in sera. The Mann-Whitney test was performed to estimate significance levels when rank scores were performed. Spearman's nonparametric test was used to calculate correlation. For these tests differences were considered statistically significant when $p < 0.05$. Diabetes frequencies were analyzed with survival curves generated with the GraphPad Prism® 4 (GraphPad Software, Inc San Diego, CA) software package. Survival curves were created using the product limit method of Kaplan and Meier and strain comparisons were performed using the log rank test.

## Results

### NOD.ABD mice develop autoimmune biliary disease comparably to NOD.c3c4 mice, but unlike NOD.c3c4 mice, NOD.ABD also develop diabetes

The NOD.c3c4 strain, which develops an autoimmune biliary disease, was originally bred with the intent to eliminate diabetes through the introgression of multiple protective B6/B10 *Idd* loci (24). We developed another NOD congenic strain, NOD.ABD, which develops a similar autoimmune liver disease to NOD.c3c4 mice, while we were testing for the effects of other genome regions on diabetes (see Materials and Methods). The *Idd* congenic regions in NOD.ABD are a subset of those present in the NOD.c3c4 strain (Fig. 1a), and the NOD.ABD mouse is only partially protected from diabetes as compared to NOD mice (Fig. 1b) whereas the NOD.c3c4 strain is completely protected from autoimmune diabetes (24). The genetic basis of the liver disease in regard to the *Idd* loci introgressed is an ongoing study and will be published in the future.

100% of NOD.ABD mice (N = 106) developed evidence of autoimmune biliary disease (in contrast to the partial penetrance of T1D in these mice), with CBD dilation, biliary epithelial proliferation and severe peri-biliary lymphocyte infiltrates virtually identical to what we have reported in the NOD.c3c4 mouse (Fig. 2a). The severity of CBD dilation increased with, and was correlated, with age (r = 0.56; P < 0.0001, Spearman's correlation). Male and female NOD.ABD mice developed disease with equal penetrance. Histologically, we quantified three parameters: 1) the number of bile ducts involved per sample, 2) the amount of biliary epithelial cell proliferation as evidenced by the formation of abnormal biliary ductules and "cysts" (end-stage, dilated ductules as seen in Fig. 2a), and 3) the amount of leucocytic infiltration/inflammation. Whereas normal NOD or B6 mice have a score of zero in each category, NOD.ABD mice had mean scores of 2.67/3, 2.75/4 and 2.75/4 for these parameters (Fig. 2e). Other histological changes found in both human PBC and in the NOD.c3c4 mouse, such as small duct damage, macrophage aggregation in the duct lumen, eosinophilic infiltration, and granuloma-like lesions were also found in older NOD.ABD mice (data not shown). Vascular injury was not seen in association with the biliary injury.

Previously we had not noted CBD in young NOD.c3c4-*scid* mice (14). As we aged these mice, however, they developed mild CBD dilation (see below, Table 1). Notably, NOD.c3c4-*scid* mice never developed any evidence of gross liver pathology (which is quite evident in NOD.ABD mice). This led us to quantitate the histological score of NOD.c3c4-*scid* mice (Fig. 2b). Although the NOD.c3c4-*scid* liver histology was not completely normal (unlike NOD-*scid* histology), it was significantly less severe than the NOD.ABD histology (Fig. 2e). A representative micrograph (Fig. 2b) shows very minor biliary epithelial duct involvement and proliferation with minimal cellular infiltrate.

### Transfer studies with NOD.ABD, NOD and NOD.c3c4-scid mice: NOD.ABD, but not NOD, splenocytes transfer biliary disease without biliary epithelial cyst formation

We used adoptive transfer of NOD.ABD spleen cells into NOD.c3c4-*scid* and NOD-*scid* mice to dissect the pathogenesis of NOD.ABD biliary disease. $40 \times 10^6$ splenocytes from diseased male or female NOD.ABD mice were transferred into NOD.c3c4-*scid* or NOD-*scid*

recipients (Table 1). The recipient *scid* mice were examined 33-43 days following transfer and scored for CBD and histological disease. Both male and female NOD.c3c4-*scid* recipients developed autoimmune biliary disease with increased CBD and histopathological disease scores (Table 1). In several cases, recipient *scid* mice became quite ill. In marked contrast, transfer of splenocytes from the same NOD.ABD donors produced no disease at all in NOD-*scid* recipients, all of which had CBD and histological scores of zero (Table 1, Fig. 2e).

One aspect of NOD.ABD disease that differs from human PBC is the presence of extensive biliary proliferation (Fig. 2a); although biliary cell proliferation is a histological characteristic of stage two PBC in the Scheuer classification in early PBC (25), it is not a prominent feature of advanced human disease. We used the transfer model to address whether biliary inflammation and duct destruction were independent from, or dependent upon, biliary cell proliferation. NOD.c3c4-*scid* mice receiving $40 \times 10^6$ NOD.ABD splenocytes were compared histologically to age matched *scid* mice that received no treatment. As shown in Fig. 2c, the recipients of NOD.ABD cells developed severe disease in a short period of time with prominent lymphocytic infiltrates. The number of biliary ducts involved, and the amount of leucocytic infiltrates, was significantly higher (P=0.0003 for each, Fig 2e) in the NOD.c3c4-*scid* mice receiving NOD.ABD cells compared to untreated NOD.c3c4-*scid*. Notably, however, the amount of proliferating epithelium was significantly less in the NOD.c3c4-*scid* mice receiving NOD.ABD cells than in NOD.ABD mice (P < 0.0001), and not significantly different from untreated NOD.c3c4-*scid* mice (P = 0.7) (Fig. 2c and "cyst" score in 2e). Higher power magnification showed that many ductules in mice receiving NOD.ABD splenocytes underwent nonsuppurative destructive cholangitis very similar to human PBC (Fig. 2d, e). These transfer studies were scored blindly by two individuals with similar results as summarized in Table 1. To test whether splenocytes from donors that do not develop ABD could cause ABD in NOD.c3c4-*scid* recipients, we used NOD spleen cell transfers as a control. Notably, there was no significant difference in the any of the histological scores between untreated NOD.c3c4-*scid* recipients and those receiving NOD spleen cells. In addition, transfer of NOD.ABD spleen cells to NOD.c3c4-*scid* recipients resulted in significantly worse ductal damage (P = 0.005) and lymphoid infiltrate (P = 0.03), but not cyst score (P = 0.08) than transferred NOD splenocytes (Fig. 2e). These results strongly suggest that NOD spleen cells do not transfer ABD.

The transfer studies demonstrate that the adaptive immune system is necessary for clinical disease in the ABD model. In addition, these studies suggest that the primary lesion mediated by the adaptive immune system is ductule damage and nonsuppurative destructive cholangitis. Since nonsuppurative destructive cholangitis arose in the transfer model independent of the development of biliary epithelial cell proliferation, it is likely that biliary epithelial cell proliferation is a secondary effect of chronic inflammation in this mouse model, rather than a primary pathological lesion. Finally, these results demonstrate that the transfer recipient must have the congenic genetic composition supporting the development of ABD in order for autoimmune biliary disease to develop.

In addition to developing biliary disease, a high proportion of *scid* recipients developed anti-PDC-E2 autoantibodies (Table 1). 7/10 and 4/4 male and female recipients, respectively,

were PDC-E2 positive by immunoblotting. Several NOD-*scid* recipients also developed anti-PDC-E2 antibodies, in the absence of disease. In contrast, 0/4 NOD.c3c4-*scid* controls had PDC-E2 antibodies. Notably, several female NOD.c3c4-*scid* (4/8) and NOD-*scid* (3/3) recipients of female NOD.ABD spleen developed diabetes in the transfer experiments (Table 1), illustrating that the NOD.c3c4-*scid* recipients were permissive for transferring T1D as well as autoimmune biliary disease.

## Increased memory CD8 T cells and enhanced inflammatory cytokine production in NOD.ABD mice

We next performed an analysis of intrahepatic cellular subpopulations in livers from 5 week old NOD.ABD mice using flow cytometry; using the ABD and TID disease-free B10.H2$^{g7}$ strain as a negative control (B10.H2$^{g7}$ mice have the chromosome 17 region containing the NOD MHC (H2$^{g7}$) introgressed onto the B10 background). Analysis of three major intrahepatic cell subsets defined by light scatter showed that NOD.ABD mice had a significantly increased proportion in the "granulocyte" light scatter gate (predominant cell subset = CD11b+, F4/80-, Gr-1+), but not macrophage (predominant cell subset = CD11b+, F4/80+) and lymphocyte (containing most B, T, NK, and NKT cells) light scatter gates compared to B10.H2$^{g7}$ mice (Supplemental Figure 1a-c). It is not clear at this time whether the increased granulocyte population is a cause or effect of ABD. Analysis of the cell subsets in the lymphoid gate showed that the percentage of CD4 T cells was decreased in NOD.ABD liver (Supplemental Fig. 2a), and the percentage of NOD.ABD CD8 T cells was significantly increased in spleens and mLNs (Supplemental Fig. 2b) as compared to B10.H2$^{g7}$ mice, although the absolute cell numbers were not different (Supplemental Figs. 2c,d). These changes resulted in an overall decreased CD4:CD8 ratio in NOD.ABD lymphoid organs (Supplemental Fig. 2e). Finally, the percentages of NK, NKT, and B cells in the intrahepatic lymphoid gate were not statistically different between NOD.ABD and B10.H2$^{g7}$ mice (Supplemental Fig. 2f). Next we examined specific CD4 and CD8 T cell subpopulations (Fig. 3a) in NOD.ABD mice. The frequency of central memory (CD44+CD62L+, Fig. 3b) and effector memory (CD44+CD62L-, Fig. 4c) CD8 T cells were significantly increased in the livers of NOD.ABD mice. This was accompanied by a decrease in naïve (CD44-CD62L+) CD8 T cells frequencies in the liver (Fig. 3d). In contrast, the frequency of naïve and memory CD4 T cells was not significantly different between the strains (Fig. 3e, f).

The inflammatory profile of the increased T cell population may influence the cytokine milieu and nature of the inflammatory response in NOD.ABD mice. Thus, we first collected sera from these mice and measured serum cytokine levels. Inflammatory cytokines such as IFNγ and TNFα were undetectable in sera from groups of 10-12 week and 17-21 week old mice (data not shown). We then evaluated cytokine production by splenic CD4 and CD8 T cells mice following stimulation with anti-CD3 and CD28 antibodies for 3 days, and compared them with cytokines produced from T cells obtained from biliary/diabetes disease-free B10.H2$^{g7}$ mice. As shown in Fig. 4a, both IFNγ and TNFα production was significantly higher from NOD.ABD CD8 T cells as compared to B10.*H2*$^{g7}$ CD8 T cells. However, the amount of these cytokines produced by NOD.ABD and B10.*H2*$^{g7}$ CD4 T cells was similar. To test if intrahepatic CD8 T cells showed similar changes, we cultured NOD.ABD or

B10.H2$^{g7}$ intrahepatic CD8 T cells with anti-CD3/CD28 and showed that the NOD.ABD intrahepatic CD8 T cells had significantly increased interferon-γ production compared to B10.H2$^{g7}$ intrahepatic CD8 T cells (Figs. 4b, c) further indicating that autoreactive CD8 T cells in NOD.ABD mice may have a prominent role in the induction of autoimmune biliary disease.

### CD8+ T cells can transfer disease, which is ameliorated by co-transfer of CD25+ T regulatory cells

Given the ability of whole spleen to transfer disease, increased inflammatory cytokine production by NOD.ABD CD8 T cells, and the demonstration of increased memory CD8 T cells in NOD.ABD livers, we next focused on transfer studies with CD8 T cells plus or minus other cell subsets. We purified CD8 T cells from NOD.ABD donors and transferred them with and without other cell subsets into NOD.c3c4-*scid* recipients (Fig. 5). Recipients of NOD.ABD CD8 T cells alone developed pronounced lymphocytic peribiliary infiltrates (Fig. 5a, d). Co-transfer of NOD.ABD CD8 T cells with CD4+CD25- T cells also resulted in significant disease (Fig. 5b, d). In marked contrast, the co-transfer of CD8 T cells with a population enriched in Tregs (CD4+CD25+ T cells) significantly ameliorated disease (P=0.03); the histological sections were only minimally abnormal (Fig. 5c, d). As a control, we transferred FACS sorted NOD CD8 T cells alone or NOD CD8 T cells plus NOD CD25-CD4 T cells into NOD.c3c4-*scid* recipients (Fig. 5d). None of the mice developed significant ABD, and the severity of the lymphoid histological score of NOD.c3c4-*scid* recipients of NOD CD8 T cells was not significantly different from the transfer of NOD.ABD CD8 T cells plus T regulatory cells (Fig. 5d). In contrast, all of the recipients of co-transferred NOD CD8 T cells plus NOD CD4+CD25- T cells rapidly developed diabetes (not shown), again showing that the NOD.c3c4-*scid* background is permissive for T1D despite the absence of diabetes in NOD.c3c4 mice.

These studies show that T regulatory cells can ameliorate ABD. It raises the question as to why the same Tregs cannot prevent the disease spontaneously in NOD.ABD mice. To begin to understand this we examined the CD25+, Foxp3+ Treg population in the liver. Although NOD.ABD mice and control mice have a similar percentage of hepatic Tregs, the overall percentage of this T regulatory cell subpopulation in the intrahepatic lymphoid population is quite low (Fig. 6). This suggests that in our transfer system Tregs may act to prevent the disease due to a much increased ratio of Treg:Teffector cell compared to the normal intrahepatic environment.

### NOD.ABD mice do not develop ANA or Anti-Smith antibodies but do develop autoantibodies to Pyruvate Dehydrogenase

We previously showed that NOD.c3c4 mice develop extensive autoantibodies including antinuclear antibodies and anti-Smith antibodies (as detected by immunoprecipitation, see Methods), and that the ability to produce these autoantibodies mapped to the *Idd9.3* congenic region on chromosome 4; mice with a B10 allele at *Idd9.3* produced more antibodies than mice with an NOD allele at this locus (15, 26). We tested NOD.ABD mice for ANAs and found that, in contrast to NOD.c3c4 mice, they did not develop significant ANA and anti-Smith antibodies (1/30 NOD.ABD mice were positive for ANA and anti-

Smith antibodies even though all mice had liver inflammation). The low incidence of ANA and anti-Smith antibodies in NOD.ABD mice was comparable to that found in the NOD strain in our lab (26). Nevertheless, NOD.ABD mice developed anti-PDC-E2 antibodies, although at a lower penetrance than in human disease. The incidence of anti-PDC-E2 antibodies rose with age and therefore with disease severity. Only 1/10 (10%) of NOD.ABD mice with a CBD score of 1 had a positive PDC-E2 autoantibody by immunoblot; compared to 9/48 (19%) of NOD.ABD mice with a CBD score of 2-3, and 21/48 (44%) with a CBD score of 4-5. The lack of generalized autoantibody formation is likely due to the presence of the NOD *Idd9.3* allele in NOD.ABD mice, which contrasts with NOD.c3c4 mice having a B10 allele at *Idd9.3* (26). Conversely, the emergence of PDC-E2 autoantibodies despite a lack of the generalized autoantibody formation in NOD.c3c4 mice points to a specific immune process involving PDC-E2 in the diseased liver. The low incidence of anti-PDC-E2 antibodies in younger (less than 20 weeks) NOD.ABD mice and the occurrence of anti-PDC-E2 antibodies with liver inflammation and damage suggests either that the PDC-E2 antibodies seen here may represent a secondary effect of biliary tissue damage or that early levels of the antibody are below detection. It is possible that since the antibody-enhancing *Idd9.3* allele is present in NOD.c3c4 mice, titers of PDC-E2 autoantibodies would be increased in younger mice and therefore more easily detected.

## Discussion

The NOD.c3c4 mouse, bred to delineate the genetic control of T1D, develops autoimmune biliary disease but no diabetes (15). Here we report a novel congenic strain, NOD.ABD that develops two organ specific autoimmune diseases, T1D and ABD. Concurrent autoimmune diseases have been reported in humans, and there have been multiple case reports of human patients with both T1D and Primary Biliary Cirrhosis. One recent analysis of multiple autoimmune syndromes demonstrated two patients with both T1D and PBC out of a cohort of 278 (27). Pietropaolo et al. also found that a similar small percentage (5.5%) of PBC patients had GAD65 autoantibodies typical of T1D (28). Notably, however, human PBC patients are typically female, while disease penetrance is the same in NOD.ABD males and females. The reduction of the chromosome 3 and 4 congenic intervals present in the NOD.ABD strain as compared to NOD.c3c4 mice reduces the number of known diabetes-resistance alleles from seven (*Idd3, Idd17, Idd10,* and *Idd18* on chromosome 3 and *Idd9.1, Idd9.2*, and *Idd9.3* on chromosome 4) to two (only *Idd10* and *Idd18*) and allows emergence of T1D, while it did not abrogate ABD. NOD.ABD mice develop ABD that is histopathologically similar to NOD.c3c4 mice and 100 % penetrant. Current studies are aimed at determining which genetic regions in the NOD.c3c4 and NOD.ABD strains are essential for the development of liver autoimmunity.

We previously published that NOD.c3c4 mice develop a wide range of autoantibodies, including early anti-PDC-E2 antibodies (14–15). We also showed that genetic control of the antinuclear and anti-Smith antibodies was localized to *Idd9.3* on chromosome 4 (26). Here we show that NOD.ABD mice do not develop ANA or anti-Smith antibodies, consistent with the removal of B10 *Idd9.3* allele from the NOD.ABD strain. In addition, the time onset of anti- PDC-E2 antibodies is different in NOD.ABD mice compared to NOD.c3c4 mice. We show here that NOD.ABD mice have an increasing penetrance of anti- PDC-E2

antibodies with age, nearing 50% in older mice. This finding suggests either that PDC-E2 antibodies might result from, rather than cause, biliary inflammation and disease, or that the *Idd9.3* region could allow for the earlier detection of PDC-E2 antibodies because *Idd9.3* facilitates increased titers. The latter possibility suggests that the penetrance of PDC-E2 antibodies could be increased by combining a B10-derived allele at *Idd9.3* with the non-NOD genetic intervals present in NOD.ABD mice.

One aspect of NOD.c3c4 pathology that does not resemble human PBC is the development of proliferative biliary epithelium. We have hypothesized that the bile duct cells proliferate in response to increased cytokines in the inflamed biliary portal areas. Here we show that liver inflammation, ductal damage and PDC-E2 antibody formation can be separated from proliferative biliary disease. As shown in Fig. 2, donor NOD.ABD splenocytes are capable of producing severe biliary disease in NOD.c3c4-*scid* recipients without biliary epithelial proliferation. These results clearly indicate that biliary damage and disease precede and can be independent from biliary epithelial proliferation. This is important because it suggests further similarities between this mouse model and human PBC. The ductule damage shown in Fig. 2d is very characteristic of human PBC.

The autoimmune biliary disease in NOD.ABD mice could represent an intrinsic biliary defect, a defect in either regulatory or effector adaptive immunity, a lesion in innate immunity, or some combination of the three. Our adoptive transfer experiments were designed to investigate these possibilities by using donors and recipients that had or lacked the non-NOD alleles required to develop ABD. The results were striking and clear cut: the recipient mice had to have an ABD-sufficient genetic background, as NOD-*scid* recipients developed no liver disease or biliary histological abnormalities despite receiving the same cells that caused overwhelming biliary disease in NOD.c3c4-*scid* recipients (Fig. 2 and Table I). This experiment demonstrated that the genetic origin of the liver "target tissue" is critical to the outcome of disease. In addition, whereas NOD.ABD splenocytes transferred diabetes into NOD.c3c4-*scid* recipients, NOD spleen and CD8 T cells were not sufficient to transfer ABD to NOD.c3c4-*scid* recipients. The inability of NOD cells to induce ABD could relate either to the lack of expanded populations of biliary reactive T cells in the NOD periphery, or to a necessary role for the ABD genetic background in the T cells in order to induce ABD. Future studies using bone marrow chimeras will aim to dissect these possibilities. We are also currently developing recipient and donor mice with individual segments of the congenic regions present in NOD.ABD mice to determine which gene or genes are required in the donor and recipient mice to successfully transfer disease.

We have noted above that several mouse models of PBC have become available in the last few years. However, it is still difficult to evaluate what is the main pathogenic feature allowing PBC in these models—or if they have a common pathogenesis. Excess adaptive immunity and defective regulatory immunity could both play a major role. Here, we clearly show a pathological role for CD8 T cells. We show that NOD.ABD CD8 T cells produce more inflammatory cytokines and that the memory fraction is increased in NOD.ABD livers —whereas CD4 T cells show no such differences from controls. In addition, NOD.ABD CD8 T cells alone can transfer disease (Fig. 5); in general in the NOD model of T1D both splenic CD4 and CD8 T cells are required for disease transfer although some CD8+ clones

can transfer the disease without CD4+ cells (29–30). Finally, NOD CD8 T cells cannot transfer disease, which shows that either the NOD T cell repertoire lacks antigen expanded biliary reactive CD8 T cells, or that genetic differences between NOD and NOD.ABD strains affect CD8 T cell autoreactivity. Importantly, we can't exclude the possibility that the increased memory fraction of CD8 T cells in the NOD.ABD liver arose elsewhere and accumulated in the liver. In terms of immune regulation, in this and other models two major cell types have emerged as candidates. The first is T regulatory cells, implicated because of liver pathology in mice lacking a functional IL-2R and in mice whose CD4 T cells cannot receive TGF-beta signaling (16, 31). The second is NKT cells, implicated by the induction of biliary disease in an NKT dependent fashion in B6 mice, and by the worsening of biliary disease in CD1d$^{-/-}$-dnTGFβRII mice (32–33). Here, we do not prove or disprove a role for either of these subsets. However, we show that co-transfer of CD25+ Tregs can ameliorate ABD in our transfer model, and that there is a paucity of FoxP3$^+$ T regulatory cells in the hepatic lymphoid population in both control and NOD.ABD mice. Given the low numbers of Tregs in the NOD.ABD hepatic environment and the fact that the liver is the main reservoir of NKT cells in the lymphoid system, we suggest it is unlikely that FoxP3$^+$ Tregs can effectively regulate pathology in unmanipulated NOD.ABD mice. In contrast, in our transfer model the ratio of Treg:Teffectors is much higher than normal, and the NOD.c3c4-*scid* recipients lack NKT cells. This leaves open the question of the *in vivo* physiological relevance of hepatic Tregs in the disease process. Given the well-known role of Tregs in T1D, we hypothesize that the reappearance of diabetes in NOD.ABD mice (compared to complete protection in NOD.c3c4 mice) could be related to decreased Treg function, whereas the biliary pathology may be related to hepatic NKT cell function combined with low numbers of Tregs in the hepatic immune microenvironment. This raises the hypothesis, which will be explored in future studies, that the different organ specific autoimmune diseases in the NOD.ABD mouse are regulated, at least in part, by distinct cellular immunological pathways in the setting of an overall NOD background.

## Supplementary Material

Refer to Web version on PubMed Central for supplementary material.

## Acknowledgments

## Abbreviations

| | |
|---|---|
| *Idd* | insulin-dependent diabetes |
| **PBC** | primary biliary cirrhosis |
| **T1D** | type 1 diabetes |
| **CBD** | common bile duct |

**PDC-E2**    Pyruvate Dehydrogenase Complex E2

**ABD**    Autoimmune biliary disease

## References

1. Gershwin ME, Ansari AA, Mackay IR, Nakanuma Y, Nishio A, Rowley MJ, Coppel RL. Primary biliary cirrhosis: an orchestrated immune response against epithelial cells. Immunol Rev. 2000; 174:210–225. [PubMed: 10807518]

2. Gershwin ME, Mackay IR, Sturgess A, Coppel RL. Identification and specificity of a cDNA encoding the 70 kd mitochondrial antigen recognized in primary biliary cirrhosis. J Immunol. 1987; 138:3525–3531. [PubMed: 3571977]

3. Van de Water J, Ansari AA, Surh CD, Coppel R, Roche T, Bonkovsky H, Kaplan M, Gershwin ME. Evidence for the targeting by 2-oxo-dehydrogenase enzymes in the T cell response of primary biliary cirrhosis. J Immunol. 1991; 146:89–94. [PubMed: 1984455]

4. Jones DE, Palmer JM, James OF, Yeaman SJ, Bassendine MF, Diamond AG. T-cell responses to the components of pyruvate dehydrogenase complex in primary biliary cirrhosis. Hepatology. 1995; 21:995–1002. [PubMed: 7705811]

5. Ichiki Y, Shimoda S, Ishibashi H, Gershwin ME. Is primary biliary cirrhosis a model autoimmune disease? Autoimmun Rev. 2004; 3:331–336. [PubMed: 15246030]

6. Kita H, Matsumura S, He XS, Ansari AA, Lian ZX, Van de Water J, Coppel RL, Kaplan MM, Gershwin ME. Quantitative and functional analysis of PDC-E2-specific autoreactive cytotoxic T lymphocytes in primary biliary cirrhosis. J Clin Invest. 2002; 109:1231–1240. [PubMed: 11994412]

7. Kita H, Lian ZX, Van de Water J, He XS, Matsumura S, Kaplan M, Luketic V, Coppel RL, Ansari AA, Gershwin ME. Identification of HLA-A2-restricted CD8(+) cytotoxic T cell responses in primary biliary cirrhosis: T cell activation is augmented by immune complexes cross-presented by dendritic cells. J Exp Med. 2002; 195:113–123. [PubMed: 11781370]

8. Shimoda S, Nakamura M, Ishibashi H, Hayashida K, Niho Y. HLA DRB4 0101-restricted immunodominant T cell autoepitope of pyruvate dehydrogenase complex in primary biliary cirrhosis: evidence of molecular mimicry in human autoimmune diseases. J Exp Med. 1995; 181:1835–1845. [PubMed: 7536796]

9. Wang AP, Migita K, Ito M, Takii Y, Daikoku M, Yokoyama T, Komori A, Nakamura M, Yatsuhashi H, Ishibashi H. Hepatic expression of toll-like receptor 4 in primary biliary cirrhosis. J Autoimmun. 2005; 25:85–91. [PubMed: 16006099]

10. Padgett KA, Selmi C, Kenny TP, Leung PS, Balkwill DL, Ansari AA, Coppel RL, Gershwin ME. Phylogenetic and immunological definition of four lipoylated proteins from Novosphingobium aromaticivorans, implications for primary biliary cirrhosis. J Autoimmun. 2005; 24:209–219. [PubMed: 15848043]

11. Zachou K, Rigopoulou EI, Tsikrikoni A, Alexandrakis MG, Passam F, Kyriakou DS, Stathakis NE, Dalekos GN. Autoimmune hepatitis type 1 and primary biliary cirrhosis have distinct bone marrow cytokine production. J Autoimmun. 2005; 25:283–288. [PubMed: 16242912]

12. Rieger R, Gershwin ME. The X and why of xenobiotics in primary biliary cirrhosis. J Autoimmun. 2007; 28:76–84. [PubMed: 17360156]

13. Prince MI, James OF. The epidemiology of primary biliary cirrhosis. Clin Liver Dis. 2003; 7:795–819. [PubMed: 14594132]

14. Irie J, Wu Y, Wicker LS, Rainbow D, Nalesnik MA, Hirsch R, Peterson LB, Leung PS, Cheng C, Mackay IR, Gershwin ME, et al. NOD.c3c4 congenic mice develop autoimmune biliary disease that serologically and pathogenetically models human primary biliary cirrhosis. J Exp Med. 2006; 203:1209–1219. [PubMed: 16636131]

15. Koarada S, Wu Y, Fertig N, Sass DA, Nalesnik M, Todd JA, Lyons PA, Fenyk-Melody J, Rainbow DB, Wicker LS, Peterson LB, et al. Genetic control of autoimmunity: protection from diabetes, but spontaneous autoimmune biliary disease in a nonobese diabetic congenic strain. J Immunol. 2004; 173:2315–2323. [PubMed: 15294944]

16. Wakabayashi K, Lian ZX, Moritoki Y, Lan RY, Tsuneyama K, Chuang YH, Yang GX, Ridgway W, Ueno Y, Ansari AA, Coppel RL, et al. IL-2 receptor alpha(-/-) mice and the development of primary biliary cirrhosis. Hepatology. 2006; 44:1240–1249. [PubMed: 17058261]

17. Gorelik L, Flavell RA. Abrogation of TGFbeta signaling in T cells leads to spontaneous T cell differentiation and autoimmune disease. Immunity. 2000; 12:171–181. [PubMed: 10714683]

18. Fraser HI, Dendrou CA, Healy B, Rainbow DB, Howlett S, Smink LJ, Gregory S, Steward CA, Todd JA, Peterson LB, Wicker LS. Nonobese diabetic congenic strain analysis of autoimmune diabetes reveals genetic complexity of the Idd18 locus and identifies Vav3 as a candidate gene. J Immunol. 2010; 184:5075–5084. [PubMed: 20363978]

19. Podolin PL, Denny P, Armitage N, Lord CJ, Hill NJ, Levy ER, Peterson LB, Todd JA, Wicker LS, Lyons PA. Localization of two insulin-dependent diabetes (Idd) genes to the Idd10 region on mouse chromosome 3. Mamm Genome. 1998; 9:283–286. [PubMed: 9530623]

20. Irie J, Wu Y, Kachapati K, Mittler RS, Ridgway WM. Modulating protective and pathogenic CD4+ subsets via CD137 in type 1 diabetes. Diabetes. 2007; 56:186–196. [PubMed: 17192481]

21. Lian ZX, Okada T, He XS, Kita H, Liu YJ, Ansari AA, Kikuchi K, Ikehara S, Gershwin ME. Heterogeneity of dendritic cells in the mouse liver: identification and characterization of four distinct populations. J Immunol. 2003; 170:2323–2330. [PubMed: 12594254]

22. Migliaccio C, Nishio A, Van de Water J, Ansari AA, Leung PS, Nakanuma Y, Coppel RL, Gershwin ME. Monoclonal antibodies to mitochondrial E2 components define autoepitopes in primary biliary cirrhosis. J Immunol. 1998; 161:5157–5163. [PubMed: 9820485]

23. Migliaccio C, Van de Water J, Ansari AA, Kaplan MM, Coppel RL, Lam KS, Thompson RK, Stevenson F, Gershwin ME. Heterogeneous response of antimitochondrial autoantibodies and bile duct apical staining monoclonal antibodies to pyruvate dehydrogenase complex E2: the molecule versus the mimic. Hepatology. 2001; 33:792–801. [PubMed: 11283841]

24. Lyons PA, Hancock WW, Denny P, Lord CJ, Hill NJ, Armitage N, Siegmund T, Todd JA, Phillips MS, Hess JF, Chen SL, et al. The NOD Idd9 genetic interval influences the pathogenicity of insulitis and contains molecular variants of Cd30, Tnfr2, and Cd137. Immunity. 2000; 13:107–115. [PubMed: 10933399]

25. Kumagi T, Heathcote EJ. Primary biliary cirrhosis. Orphanet J Rare Dis. 2008; 3:1. [PubMed: 18215315]

26. Irie J, Wu Y, Sass DA, Ridgway WM. Genetic control of anti-Sm autoantibody production in NOD congenic mice narrowed to the Idd9.3 region. Immunogenetics. 2006; 58:9–14. [PubMed: 16425035]

27. Teufel A, Weinmann A, Kahaly GJ, Centner C, Piendl A, Worns M, Lohse AW, Galle PR, Kanzler S. Concurrent autoimmune diseases in patients with autoimmune hepatitis. J Clin Gastroenterol. 2010; 44:208–213. [PubMed: 20087196]

28. Pietropaolo M, Peakman M, Pietropaolo SL, Zanone MM, Foley TP Jr, Becker DJ, Trucco M. Combined analysis of GAD65 and ICA512(IA-2) autoantibodies in organ and non-organ-specific autoimmune diseases confers high specificity for insulin-dependent diabetes mellitus. J Autoimmun. 1998; 11:1–10. [PubMed: 9480718]

29. Wicker LS, Miller BJ, Mullen Y. Transfer of autoimmune diabetes mellitus with splenocytes from nonobese diabetic (NOD) mice. Diabetes. 1986; 35:855–860. [PubMed: 3525284]

30. Graser RT, DiLorenzo TP, Wang F, Christianson GJ, Chapman HD, Roopenian DC, Nathenson SG, Serreze DV. Identification of a CD8 T cell that can independently mediate autoimmune diabetes development in the complete absence of CD4 T cell helper functions. J Immunol. 2000; 164:3913–3918. [PubMed: 10725754]

31. Oertelt S, Lian ZX, Cheng CM, Chuang YH, Padgett KA, He XS, Ridgway WM, Ansari AA, Coppel RL, Li MO, Flavell RA, et al. Anti-mitochondrial antibodies and primary biliary cirrhosis in TGF-beta receptor II dominant-negative mice. J Immunol. 2006; 177:1655–1660. [PubMed: 16849474]

32. Chuang YH, Lian ZX, Yang GX, Shu SA, Moritoki Y, Ridgway WM, Ansari A, Kronenberg M, Flavell RA, Gao B, Gershwin ME. Natural killer T cells exacerbate liver injury in a transforming growth factor beta receptor II dominant-negative mouse model of primary biliary cirrhosis. Hepatology. 2008; 47:571–580. [PubMed: 18098320]

33. Mattner J, Savage PB, Leung P, Oertelt SS, Wang V, Trivedi O, Scanlon ST, Pendem K, Teyton L, Hart J, Ridgway WM, et al. Liver autoimmunity triggered by microbial activation of natural killer T cells. Cell Host Microbe. 2008; 3:304–315. [PubMed: 18474357]
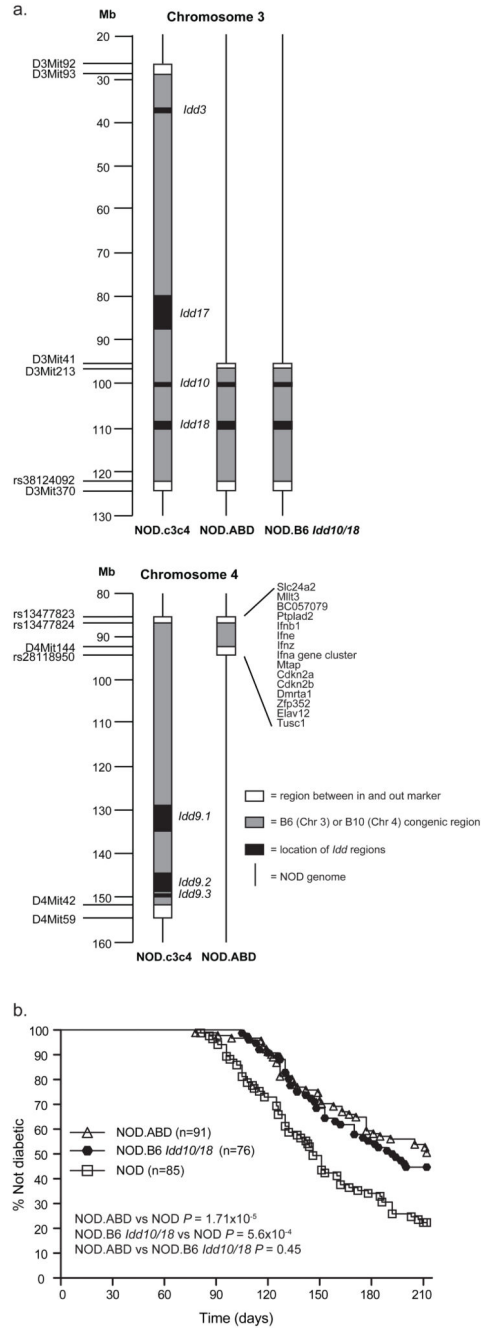
**Figure one. NOD.ABD mice develop T1D at reduced penetrance compared to NOD mice and at an equal frequency to NOD.B6 *Idd10/18* mice.**
(a) Genetic characterization of NOD.ABD mice showing a reduced number of T1D protective B6- and B10-derived *Idd* regions as compared to NOD.c3c4 mice. (b) NOD, NOD.ABD, and NOD.B6 *Idd10/18* female mice were maintained under SPF conditions and monitored weekly for diabetes by urine monitoring. The *P* value was obtained by comparing the survival curves using the log-rank test.
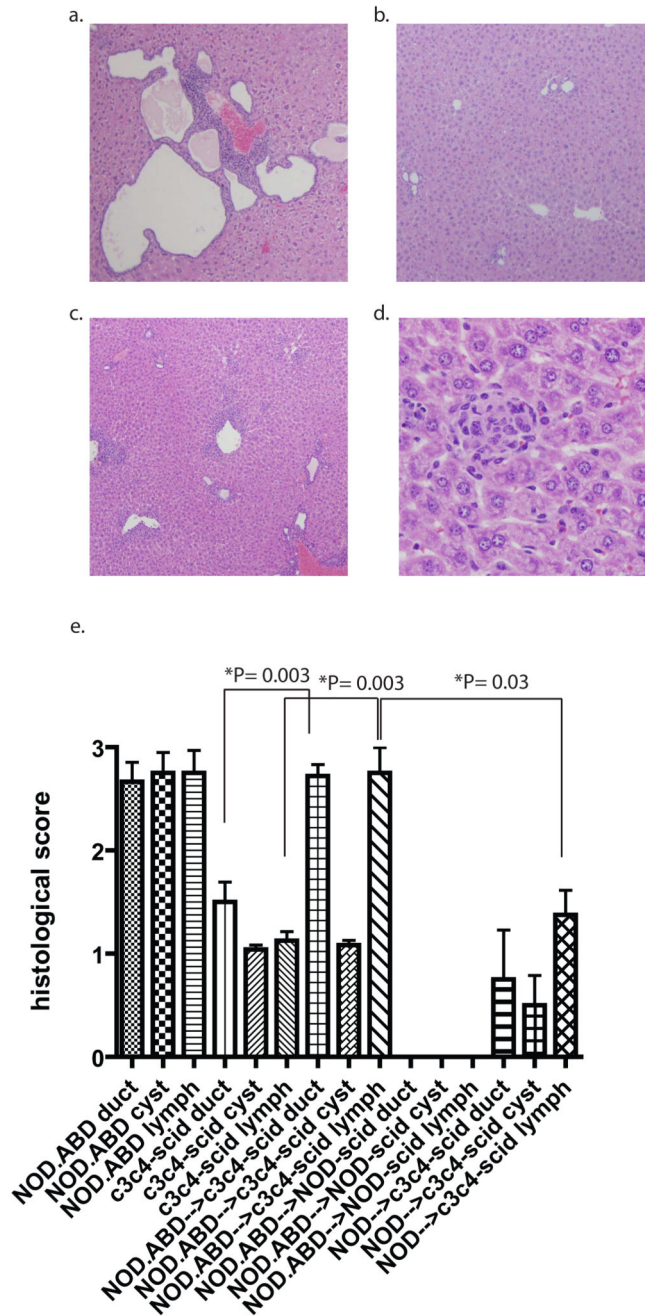
e.



**Figure two. Biliary disease in NOD.ABD mice and disease transfer to NOD.c3c4-*scid* recipients.**
(a) histological examination (4x) of 120 day NOD.ABD mice shows leucocytic
inflammation and biliary cell proliferation/cyst formation. (b) NOD.c3c4-*scid* mice show
very minimal leucocytic infiltrates and minimal biliary ductule proliferation (4x). (c)
Significant leucocytic infiltration and duct damage, but not biliary epithelial proliferation, in
NOD.c3c4-*scid* recipients of NOD.ABD splenocytes (4x). $40 \times 10^6$ splenocytes from 117 day
old NOD.ABD mice were transferred into 43 day old NOD.c3c4-*scid* recipients. 30 days
later the mice were harvested and liver sections taken for histological analysis. (d) High

power magnification (40x) showing nonsuppurative destructive cholangitis in NOD.c3c4-*scid* recipients. (e) Blinded histological scoring of ductule involvement, cyst formation, and leucocytic infiltrates in 120 day old NOD.ABD mice (n= 12), 74 day old NOD.c3c4-*scid* mice (n= 12), 74 day old NOD.c3c4-*scid* recipients of NOD.ABD splenocytes (n= 18), 85 day old NOD-*scid* recipients of $40\times10^6$ NOD.ABD splenocytes (n=6), and 78 day old NOD.c3c4-*scid* recipients of $40\times10^6$ NOD splenocytes (n=4). Significance assessed using the Mann-Whitney test.

**Figure three. Increased hepatic CD8 effector/central memory T cells in NOD.ABD mice.**
Lymphocytes were isolated from liver, spleen and mLN of 5 week old NOD.ABD and
B10.H2$^{g7}$ mice. Cells were stained with FITC-CD44, PE-CD62L, PE-Cy5-CD8, APC-
TCRβ and APC-Cy7-CD4. Frequencies of CD44$^-$CD62L$^+$, CD44$^+$CD62L$^-$, CD44$^+$CD62L$^+$
in TCRβ$^+$CD4$^+$ or TCRβ$^+$CD8$^+$ T cells were analyzed by flow cytometry. Representative
expression of CD44 and CD62L on CD4 and CD8 T cells are shown in (a). The frequencies
of each CD4 or CD8 T cell subpopulation are shown in (b-f). Data are shown as the means ±
SD. Each group included 7 to 8 mice (*, NOD.ABD vs. B10.H2$^{g7}$, p<0.05).
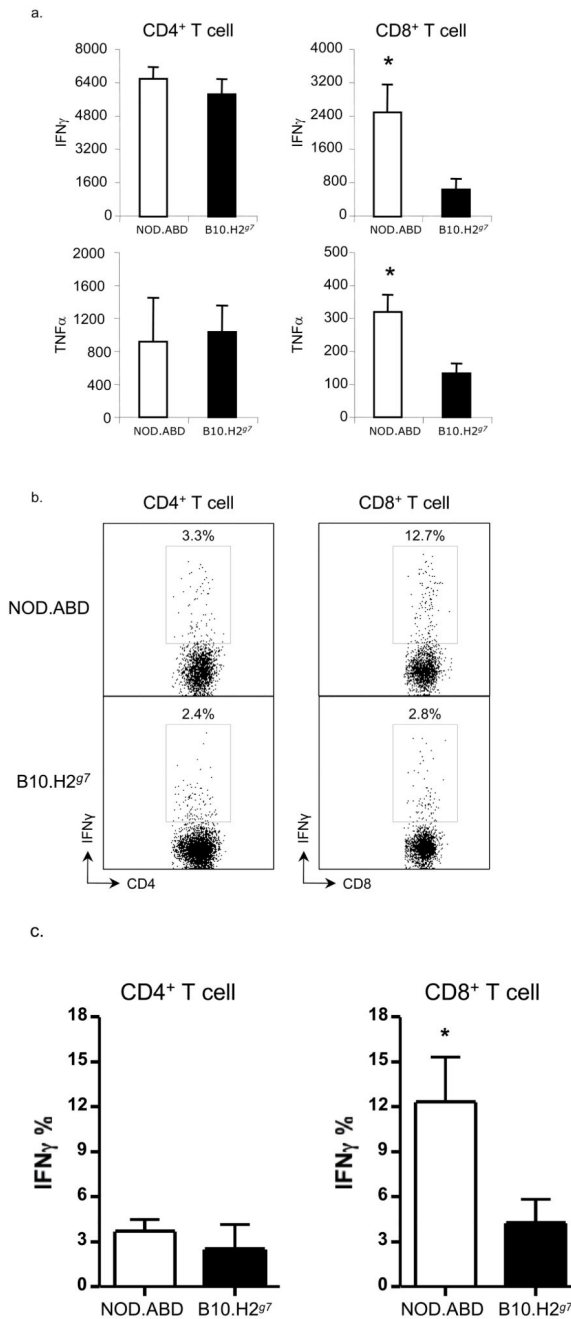
**Figure four. Increased inflammatory cytokine production by NOD.ABD CD8 T cells.**
(a) CD4 and CD8 T cells were purified from NOD.ABD and control B10.H2$^{g7}$ splenocytes as described in Materials and Methods, and $1 \times 10^5$ cells cultured with or without CD3 and CD28 antibodies at 37°C for 3 days. Concentrations of IFN-γ and TNF-α were determined by CBA (see Materials and Methods). Data represent the average values of triplicate samples ± SD and were consistent in two repetitions. (*, p<0.05, NOD.ABD vs. B10.H2$^{g7}$). (b,c) Liver lymphoid cells were isolated and stained intracellularly as described in the Materials and Methods. The frequency of IFN-γ positive cells in CD4$^+$TCRβ$^+$ and CD8$^+$TCRβ$^+$ cell

populations were analyzed by flow cytometry. One representative example of IFN-γ in CD4^{+} and CD8^{+} T cells is shown in (b). The frequencies of IFN-γ in CD4^{+} and CD8^{+} T cells are shown in (c). Data are shown as the means ± SD. Each group included 4 mice (*, NOD.ABD vs. B10.H2$^{g7}$, p<0.05).
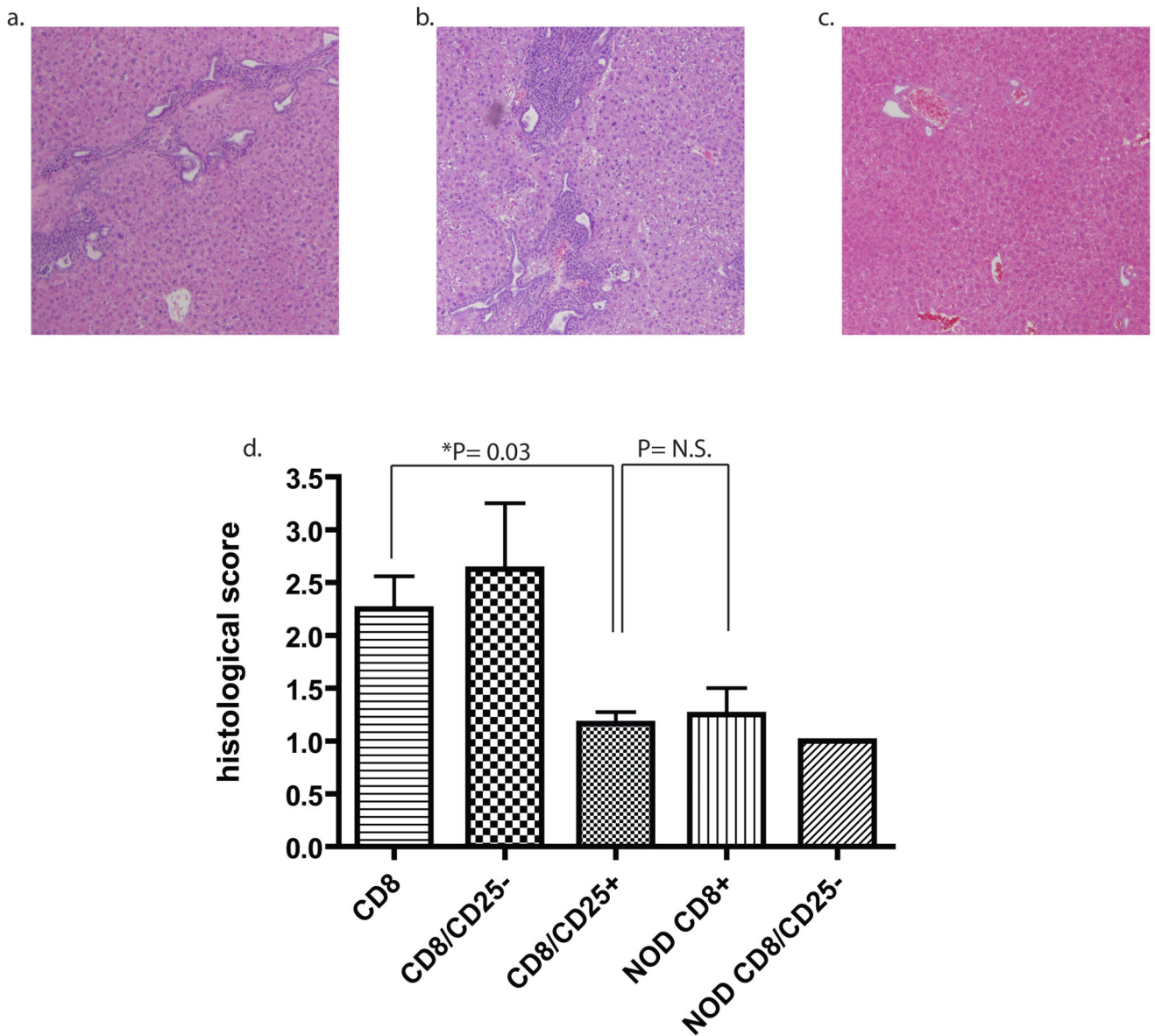
**Figure five. NOD.ABD but not NOD CD8 T cells transfer disease to NOD.c3c4-*scid* recipients; disease transfer ameliorated by co-transfer of Tregs**

(a) NOD.ABD CD8 T cells (2-4 x 10$^6$) were purified by FACS or MiniMACS from NOD.ABD donors and transferred into NOD.c3c4-*scid* recipients aged 44-58 days. After 2 months the recipients were evaluated histologically for disease. (b,c) Recipient NOD.c3c4-*scid* received 1x10$^6$ NOD.ABD CD4+CD25- (b) or CD4+CD25+ (c) cells co-transferred with the CD8 T cells. Mice were sacrificed after two months and assessed for histological evidence of disease. (d) Summary graph of separate experiments using FACS or MiniMACS sorted NOD.ABD CD8 T cells (total n = 6), NOD.ABD CD8 T cells plus CD4+CD25- T cells (total n = 4), NOD.ABD CD8 T cells plus CD4+CD25+ T cells (total n = 6), NOD CD8 T cells (n=4) or NOD CD8 T cells plus NOD CD+CD25- T cells (n = 3) cells

transferred into NOD.c3c4-*scid* recipients as in (a) and (b). P values calculated by Mann-Whitney test.
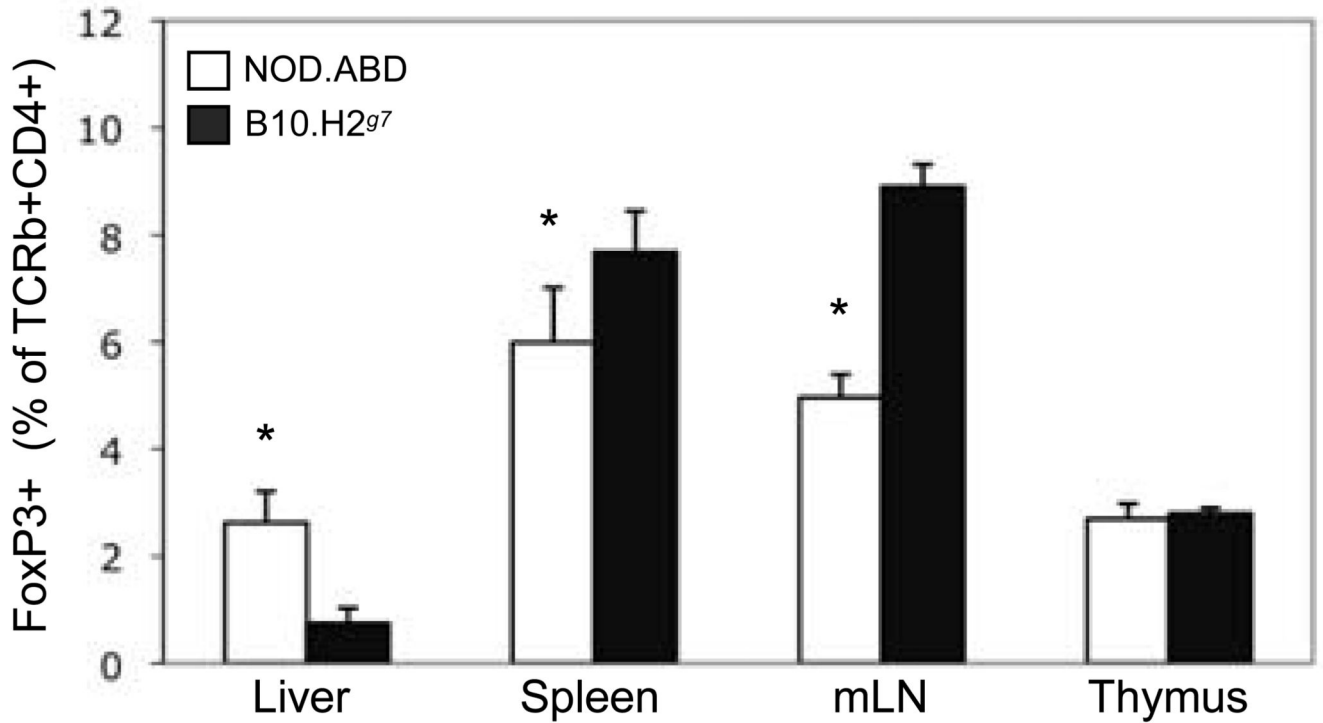
**Figure six. NOD.ABD CD25$^+$FoxP3$^+$ Treg cells are decreased in spleen but increased in liver compared to controls.**
Intrahepatic, splenic, mesenteric and thymic lymphocytes from five-week-old NOD.ABD and control B10.H2$^{g7}$ mice were isolated as described in the Material and Methods. Cells were surface stained with FITC-CD25, PE-Cy5-CD8, APC-TCRβ and APC-Cy7-CD4 and stained intracellularly with PE-FoxP3. The frequency of CD25$^+$FoxP3$^+$ cells within the TCRβ$^+$CD4$^+$ population is shown as the mean ± SD. Each group included 7 to 8 mice. (*, NOD.ABD vs. B10.H2$^{g7}$ mouse group, p<0.05).